

Abnormalities in whisking behaviour are associated with lesions in brain stem nuclei in a mouse model of amyotrophic lateral sclerosis

Robyn A Grant^a, Paul S Sharp^{b,c}, Aneurin J Kennerley^b, Jason Berwick^b, Andy Grierson^c,
Tennore Ramesh^{c*}, Tony J Prescott^{b*}

a Division of Biology and Conservation Ecology, Manchester Metropolitan University, Manchester, UK (+44 161 247 6210)
robyn.grant@mmu.ac.uk (corresponding author)

b Department of Psychology, University of Sheffield, Sheffield, UK
*t.j.prescott@sheffield.ac.uk

c Department of Neuroscience, University of Sheffield, Sheffield, UK
*t.tamesh@sheffield.ac.uk

*Joint last author

Abstract

(250 words)

The transgenic SOD1^{G93A} mouse is a model of human amyotrophic lateral sclerosis (ALS) and recapitulates many of the pathological hallmarks observed in humans, including motor neuron degeneration in the brain and the spinal cord. In mice, neurodegeneration particularly impacts on the facial nuclei in the brainstem. Motor neurons innervating the whisker pad muscles originate in the facial nucleus of the brain stem, with contractions of these muscles giving rise to “whisking” one of the fastest movements performed by mammals.

A longitudinal study was conducted on SOD1^{G93A} mice and wild-type litter mate controls, comparing: i) whisker movements using high-speed video recordings and automated whisker tracking, and ii) facial nucleus degeneration using MRI. Results indicate that while whisking still occurs in SOD1^{G93A} mice and is relatively resistant to neurodegeneration, there are significant disruptions to certain whisking behaviours, which correlate with facial nuclei lesions, and may be as a result of specific facial muscle degeneration. We propose that measures of mouse whisker movement could potentially be used in tandem with measures of limb dysfunction as biomarkers of disease onset and progression in ALS mice and offers a novel method for testing the efficacy of novel therapeutic compounds.

Keywords

Facial Nucleus, Active Sensing, Vibrissae, Motor Neuron Disease, SOD1 mouse

Highlights

- Whisking is relatively resistant to neurodegeneration
- However, specific whisker movements, especially retraction velocity, are impacted by disease progression at P120.
- These behaviour changes are correlated to facial nucleus decline
- And likely to be caused by degeneration of the type ii, white muscle fibers in the caudal facial muscles
- We conclude that studying the facial musculature and whisking behaviours will give new insights in to neurodegenerative diseases.

1. Introduction

Amyotrophic lateral sclerosis (ALS) is an adult-onset progressive neuromuscular disorder that leads to degeneration of motor neurons in the motor cortex, brain stem and spinal cord, causing progressive weakness in limbs and difficulties with walking, speaking and swallowing. The extensively used SOD1^{G93A} mouse model of ALS, harbours a Gly93 to Ala amino acid substitution, and has been validated using biochemical and behavioural tests; however, the exact mechanism causing selective motor neuron degeneration is unknown (Robberecht and Philips 2013). The loss of motor neurons results in muscle paralysis; however, several studies have shown the degeneration of neuromuscular junctions and muscles to occur prior to motor neuron degeneration (David et al. 2007; Valdez et al. 2012). ALS causes significant changes throughout, but not restricted to, the pyramidal motor system, including, the nigrostriatal system, the neocortex, allocortex and the cerebellum (Geser et al. 2008). However, MRI studies have only found evidence for neurodegeneration in the motor nuclei of the brainstem, rather than motor cortex (Nimchinsky et al. 2000; Marcuzzo et al. 2011; Zang et al 2004). In the brainstem, neurodegeneration is particularly evident in the facial nucleus with reports that, in mice, up to 50% of the neurons in this nucleus are lost by the 120th post-natal day (P), compared to ~10% losses in the oculomotor and hypoglossal nucleus (Nimchinsky et al. 2000; Zang et al 2004).

In mice, the facial nerve originates within the facial nucleus and innervates both the intrinsic and extrinsic muscles of the mystacial pad. In particular, motor neurons that innervate the mystacial pad muscles are mainly found in the lateral subnucleus of the facial nucleus (Klein and Rhoades 1985). Intrinsic muscles form a sling around each whisker follicle and actuate individual vibrissae from within the mystacial pad (Dorfl 1982). Small units of motoneurons are thought to innervate the intrinsic muscles, with about 25-30 motoneurons per whisker follicle (Klein and Rhoades 1985). The extrinsic muscles are external to the pad and generate whole pad movements, such as the *m. Nasolabialis* and the *m. Maxillolabialis* that cause retraction movements of the vibrissae (Berg et al. 2003; Dorfl 1982; Grant et al. 2013; Haidarliu, 2010). Through contractions of the intrinsic and extrinsic muscles, the whiskers show rhythmic bouts of protractions and retractions, referred to as *whisking*, that are among the fastest movements performed by mammals (Mitchinson et al. 2011; Vincent 1912; Wineski 1985). The vibrissal motor neurons in the facial nucleus receive input from multiple

brain regions, including motor cortex, and thus constitutes the final common motor path for whisker control.

Behavioural studies in ALS mice have been extensively used for the development of drug treatments for ALS, but have mainly focussed on locomotion thus far, such as gait analyses and rotorod tests (Klivenyi et al. 1999; Knippenberg et al. 2010; Mead et al 2011; Weydt et al 2003; Wooley et al. 2005;). However, locomotion can be hard to quantify and often requires training on a particular task. In light of the impact of neurodegeneration on the facial nucleus, this paper aims to address whether measurements of whisker movements might provide a reliable quantification of disease onset and progression. In addition, assessing the impact of neurodegeneration on vibrissal movement in the SOD1^{G93A} mouse could lead to an improved understanding of rodent whisking motor control, which is an important model system for understanding the control of rhythmic movements in mammals. An understanding of the effects of neurodegeneration on whisker movement in these mice could therefore lead to advances in both fundamental motor neuroscience and in our understanding of ALS.

This study examines the relationship between facial nuclei lesions and whisker behaviour. We provide an analysis of whisker movements in SOD1^{G93A} mice and of age-matched, non-transgenic (Ntg) littermates using high-speed video recordings and automatic whisker tracking. Histology of the mystacial pads qualitatively compares the musculature between SOD1^{G93A} and Ntg mice by staining for cytochrome oxidase, and the facial nucleus is imaged using MRI. Our results indicate that lesions in the facial nuclei results in a significant disruption of whisking behaviour, which provides an early behavioural biomarker of disease that has not previously been reported.

2. Materials and methods

2.1. Animals

Mice were originally obtained from the Jackson Laboratory, B6SJL-Tg (SOD1-G93A)1Gur/J (stock number 002726), and were subsequently backcrossed onto the C57Bl/6 background (Harlan UK, C57Bl/6 J OlaHsd) for >20 generations (Mead et al, PLOS one 2011). Our model, on a defined inbred genetic background, shows no effect of sex or litter of origin on survival (Mead et al, PLOS one 2011). These transgenics have an average survival of 140

days, slightly longer than the outbred B6SJL-Tg (SOD1-G93A)1Gur/J (stock number 002726) strain (Mead et al, PLOS one 2011). In the first study, five SOD1^{G93A} mice and five age-matched wild-type littermate control mice (Ntg) were filmed roaming in an open arena at postnatal day (P) 60, P90 and P120 (± 5 days). At P120 two SOD1^{G93A} mice and their littermate controls were sacrificed to examine their facial muscles further. In the second study, at P30, P60, P90 and P120 (± 3 days), five SOD1^{G93A} mice and five control mice (Ntg) were imaged in a 7 Tesla magnet, to measure loss of pelvic muscle volume and to assess the development of facial nuclei lesions. They were also filmed in an open arena three days post imaging, as in Study 1. All the animals were female kept on a 12:12 light schedule at 22°C, with water and food ad libitum. All procedures were approved by the local Ethics Committee and UK Home Office, under the terms of the UK Animals (Scientific Procedures) Act, 1986.

2.2. Behaviour Recordings

High-speed digital video recordings were made using a Photron Fastcam PCI camera, recording at 500 frames per second, shutter-speed of 0.5ms, and resolution of 1024x1024. The camera was suspended from the ceiling, above a custom-built rectangular (40cm x 40cm) viewing arena with a glass floor, ceiling, and end-wall.

The mice were recorded at P30 (for the second study only), P60, P90 and P120 on two consecutive days. Video data was collected in near darkness using an infrared light box (for Study 1) or normal spectrum lightbox (for Study 2) for illumination. Multiple 1.6 second video clips were collected opportunistically (by manual trigger) when the animal moved beneath the field of view of the camera. Approximately 24 clips were collected from each animal per day. One to two clips from each day were selected per mouse (giving around $n=80$ clips per day in total) according to a selection criteria. These clips were selected when the mouse was clearly in frame, both sides of the face were visible, the head was level with the floor (no extreme pitch or yaw), the whiskers were not in contact with a vertical wall and the mouse was clearly moving forward. In each selected clip the mouse snout and whiskers were tracked, using the BIOTACT Whisker Tracking Tool (Perkon et al., 2011). The tracker semi-automatically finds the orientation and position of the snout, and the angular position (relative to the midline of the head), of each identified whisker. Tracking was validated by manually inspecting the tracking overlaid on to the video frames (See Figure 1 a and c). Clips from Study 1 were more successfully tracked than in Study 2, owing to a greater contrast of

the video footage by using an infrared lightbox. This gave rise to a larger behavioural sample size in Study 1 (P120:n=87, P90:n=69, P60:n=72) than Study 2 (P120:n=34, P90:n=37, P60:n=32, P30:n=39), although the results agree between the two studies (see Results section).

Analysis focussed on using the movement of the entire whisker field on each side of the snout using a measure of mean angular position calculated as the unsmoothed mean of all the tracked whisker angular positions on each side, in each frame (see Grant et al. 2012, and the two examples shown in Figure 1 b and d). Whisker *offset* was calculated as the mean angular position for each clip. Mean angular *retraction* and *protraction velocities* were calculated from the angular position, as the average velocity of all the backward (negative) whisker movements, and forward (positive) whisker movements, respectively. These measures were all averaged to give a mean value per clip, and each side (left and right) was also averaged together. Whisk *frequency* was estimated using an autocorrelogram of the tracked angular position. Specifically, the time series of whisker angles for each side was first smoothed using a zero-phase low-pass filter (boxcar) with a cut-off frequency of 16 Hz which is well above the highest expected whisking frequency and removes the high-frequency information. The first peak (maximum) in the autocorrelation of this smoothed time series was then identified automatically to give a first estimate of signal period. This estimate was then refined by gradient ascent on the unsmoothed autocorrelation series to locate the nearest peak to that found automatically in the smoothed series. To estimate the *amplitude* the mean value was removed from the whisking angle time series and the root mean square value was computed to give the root-mean-square (RMS) whisking amplitude. These time series were approximately sinusoidal, so the “peak-to-peak whisking amplitude” was estimated by multiplying the RMS whisking amplitude by $2\sqrt{2}$ (Chatfield, 2003). This estimate of amplitude is reasonably robust to departures from a purely sinusoidal pattern. *Locomotion velocity* was calculated as the speed of the movement forward by the animal, as a mean over the clip, using the pixel information from the nose tracking (see the yellow head outline in Figure 1a and c) and calibrated, using a calibrator tool measured using the open source video tracking toolbox ‘Tracker’ (Tracker 4.80, Douglas Brown 2013, www.cabrillo.edu). All the whisker and locomotion data was distributed normally so parametric statistical tests were carried out throughout, more information can be found in the results section.

2.3. Muscle Staining

In study 1, two SOD1^{G93A} and two Ntg mice were also sacrificed for qualitative examination of their facial musculature. The mystacial pads were removed bilaterally, by cutting down the sagittal plane and cutting around each pad (about 2 mm each side of the pad). Any pieces of bone were removed from the pads and they were placed flat between stainless steel grids in perforated plastic histology cases (Medex Supply) to prevent curling. The histology cases were then put in a solution of 100ml of phosphate buffer (PB) pH=7.4 followed by a mixture of 2.5% glutaraldehyde and 0.5% paraformaldehyde and refrigerated for 2 days. They were transferred into a solution of 20% sucrose in 0.1M Phosphate buffer pH 7.4 for 2 days.

After fixing, each of the pads was sectioned with a *microcosm cryostar* cryostat into 40 µm slices. The eight pads (from four animals) were sliced tangentially. All slices were stained for CCO activity (see Haidarliu et al. 2010) as follows. The slices were floated in a solution of 10 ml of 0.1 M PB containing 0.75 mg cytochrome c, 40 µl catalase solution and 5 mg diaminobenzidine (DAB) and 0.5 ml distilled water. They were then placed in an incubator at 37°C on a shaking platform for 2 hours until the stain developed. The slices were then rinsed in 0.05 M PB, mounted and left to air dry briefly before coverslipping with Entellan. Figures of the stained musculature were prepared from digital images. A Zeiss Lumar V12 microscope was used to obtain the images, at magnification 12x to image the whole pad, and 150x in close-up photographs. Images were collected in Axiovision and exported as .jpg images. Only small adjustments in contrast and brightness were made to the figures.

2.4. Magnetic Resonance Imaging

Five female transgenic C57Bl/6 SOD1^{G93A} and five age matched non-transgenic littermates were blind imaged in a 7 Tesla magnet (Bruker BioSpec^{AVANCE}, 310mm bore, MRI system B/C 70/30), with pre-installed 12 channel RT-shim system (B-S30) and fitted with an actively shielded, 116mm inner diameter, water cooled, 3 coil gradient system (Bruker BioSpin MRI GmbH B-GA12. 400mT/m maximum strength per axis with 80µs ramps) to assess pelvic muscle volumes and MR signal intensity of the facial nucleus at the 30, 60, 90 and 120 day time points.

Animals were placed in a custom built Perspex magnet capsule and imaged under gaseous anaesthesia (1–1.5%, flow rate 0.8–1.0 L/min continuous inhalation through a nose cone). Anaesthetic level was controlled on the basis of respiratory parameters; monitored using a

pressure sensitive pad placed under the subject's chest (SAII Model 1025 monitoring and gating system). Inside the capsule, a non-magnetic ceramic heated hot air system (SAII - MR-compatible Heater System for Small Animals) and rectal probe, integrated into the physiological monitoring system maintained the temperature of the animal. All animals were euthanized at the 120 day time point.

A ^1H birdcage volume resonator (Bruker, 300MHz, 1kW max, outer diameter 114mm/ inner diameter 72mm), placed at the iso-centre of the magnet was used for both RF transmission and reception. A workstation configured for use with ParaVision™ 4.0 software operated the spectrometer. Following field shimming, off-resonance correction and RF gain setting a tri-plane FLASH sequence (TR=100ms, TE=6ms, Flip angle =30°, Av=1, FOV=40mm*40mm, Slice thk=2mm, Matrix=128*128) was used for subject localisation. From this a fast (~5min) 3D FISP sequence (TR=8/1200ms, TE=4ms, FOV=40mm*40mm*40mm, Matrix=256*256*128) allowed low SNR visualisation of the hind limb area and thus planning of 21 axial high SNR single Spin Echo images (TR=3200ms, TE=7.5ms, Av=1, FOV=40mm*40mm, Slice thk=1mm, Matrix=256*256) covering the entire lower hind limb and pelvic region. No fat suppression was used to maximise muscle/fat contrast difference for easy segmentation.

For data processing, a macro built into ParaVision 4.0 was used for manual segmentation of muscle from fat and bone across all slices in 3 regions (the left and right hind limb and the pelvic region). Using the scan FOV setting and the slice thickness allowed for volume conversion of segmented data. The mean and standard error for each group (Sod1 and Ntg) at each time point was calculated in GraphPad Prism.

Signal intensity within the facial nucleus was assessed using a sagittal high SNR single Spin Echo image (TR=3200ms, TE=7.5ms, Av=1, FOV=40mm*40mm, Slice thk=1mm, Matrix=256*256). Facial nucleus images in the MR data were confirmed using the mouse brain in stereotactic coordinates (Paxinos and Franklin 2008). Once subjects had been subdivided into control and SOD1 groups two Region of Interests (ROIs) were selected and applied to all images across the time points; the first over the facial nucleus and the second within the white matter of the brainstem. The latter ROI was used to normalise the signal within the facial nucleus across time.

3. Results

3.1. Study 1: Time course of changes to whisking behavior in SOD1^{G93A} mice

3.1.1. *Locomotion and whisking behaviors are affected in SOD1^{G93A} mice*

Locomotion and whisking behaviors are affected during disease progression. All the whisker variables that showed significant changes by P120 can be seen in Figure 2. In particular, by P120, the SOD1^{G93A} mouse whiskers are held further back (have lower offset values), move more (have larger amplitude whisks), move slower (have lower frequencies) and retract faster (have larger retraction velocities). In addition, locomotion speeds are much slower throughout in the SOD1^{G93A} mice. Protraction velocity was not significantly affected and, therefore, will not be included in further analyses. Between-ANOVA tests compared the locomotion and whisking behaviors between the SOD1^{G93A} and Ntg mice at each time point to confirm these observations, significant results ($p < 0.05$) are indicated on Figure 2 with asterisks (*), and can also be seen in Table 1 for the P120 time point. While whisking behavior is impacted most, on more whisker variables, at P120, whisker offset and retraction velocity are both significantly affected at two time points, and locomotion is impacted throughout, from P60. The analysis was also conducted with the mouse identity as a covariate, to see if the differences between individuals could account for the differences in variables. Table 1 shows the results of this analysis at P120 and confirms earlier statistics, implying that the differences in locomotion and whisker variables are as a result of the disease rather than differences in individuals. Results at the P120 time-point for all of the variables can also be seen graphically for each animal in the Supplementary material (Supplement 2).

As whisking and locomotion are believed to be closely coupled (Grant et al. 2012), a further analysis was conducted to determine whether it is the declining locomotion abilities or disease progression that is driving the differences in whisking behaviour. A multivariate ANOVA was conducted with locomotion speed introduced as a covariate to control for its effects on whisking behaviour. Table 1 shows the results from this analysis. Statistics confirm that there are still differences in whisking behaviour between the SOD1^{G93A} and control mice, indicating that whisker variables do change irrespective of locomotion speed. This suggests that it is likely to be the disease progression, rather than simply the declining locomotion levels that account for the changes in whisking variables. To further assess

whether disease progression is affecting whisking behaviour, the muscle staining results will also be considered.

Table 1: ANOVA analysis of the locomotion and whisking variables at P120, with disease presence (Sod1 or Ntg) as the between-factor. Additional analyses conducted with mouse identity and locomotion as covariates can also be seen.

	Loco. speed	Offset	Protraction Velocity	Retraction Velocity	Frequency	Amplitude
Sod1 mean	0.46±0.13	89.90±8.45	1.52±0.178	0.32±0.16	12.18±6.93	42.42±9.14
Ntg mean	0.77±0.23	99.35±7.04	1.56±0.21	0.26±0.13	17.97±7.92	35.97±6.46
F (1, 86)	63.422	31.140	0.796	4.320	13.196	13.777
p-value	<0.001**	<0.001**	0.375 n.s	0.041*	<0.001**	<0.001**
Mouse covar.^a	**	**	n.s	**	**	**
Loco. covar.^b	n.a.	**	n.s	n.s	**	**

** indicates where $p < 0.001$

* indicates where $p < 0.05$

n.s indicates not significant ($p > 0.05$)

n.a indicates analysis not applicable

a. Mouse identity is used as a covariate in the ANOVA analysis, significance is indicated with the asterisks

b. Locomotion is used as a covariate in the ANOVA analysis, significance is indicated with the asterisks

3.1.2. Muscle staining is affected in *SOD1^{G93A}* mice

Muscle staining results are purely qualitative in this instance and applied to confirm our behavioural findings. At a first glance, the musculature does not look significantly affected in the *SOD1^{G93A}* mice. However, on closer inspection, the both the more caudal areas of the muscle pad and the intrinsic muscles seem slightly reduced and darker in the *SOD1^{G93A}* mouse (compare, especially the more caudal areas in figure 3a, with equivalent areas in figure 3d). In particular, these are the caudal extrinsic muscles (*M. nasolabialis* and *maxillolabialis*), named the superficial retracting muscles as they control the retraction movements of the whiskers. A close-up look of the superficial retraction muscles in Fig 3c and f, shows that while the Ntg mice show striated muscle fibers of red, pink and white (Figure 3c), the *SOD1*

G^{93A} mice only show the darker muscle fibers, red and pink (Figure 3f). This suggests that there is a decrease of Type ii, white muscle fibers in $SOD1^{G^{93A}}$ mice, in the caudal superficial retracting muscles and can be seen even clearer in Figure 4. Reduction of these fibres might well explain the changes in retraction velocity behaviour that have been observed in the $SOD1^{G^{93A}}$ mice.

Overall, the whisker muscles of the $SOD1^{G^{93A}}$ pad seem slightly reduced and darker than that of the Ntg mice (Figure 3a and d); however, close-ups of the intrinsic muscles (Figure 3b and e) do not show any clear differences between the $SOD1^{G^{93A}}$ and Ntg mice. There might be a tendency for the $SOD1^{G^{93A}}$ mice to have less lighter muscle fibres throughout the pad, but slices from these four animals only clearly shows a decline in the white muscles of the caudal superficial retracting extrinsic muscles.

3.2. Study 2: Disease progression effects on whisking behavior and Facial Nucleus

3.2.1. Validating whisker behaviours in $SOD1^{G^{93A}}$ mice

As different mice were used in the second study, the behaviour findings were confirmed as before (compare Figure 2 to Figure 5). The visual lightbox used in these behavioural recordings did not give as clear images, causing the tracking program to fail on more of the clips, leading to a reduction in tracked clips. The behavioural findings were confirmed again in these mice and showed similar patterns, although results were slightly weaker than those in Study 1 due to lower sample numbers (Figure 5). By P120 $SOD1^{G^{93A}}$ mice were similarly slower, with their whisker held further back, moving more, at a slower frequency, with faster retractions.

3.2.2. Pelvic muscle volume and Facial Nucleus MRI signals decline in $SOD1^{G^{93A}}$ mice

$SOD1^{G^{93A}}$ mice show a decline in pelvic muscle volume throughout the testing period from P30 to P120. This can be clearly seen in the MR images in Figure 6a. They also have a large percentage change in the difference in MR signal of the Facial Nucleus compared to the surrounding area. This difference can be seen from P60 to P120 (Figure 6b). Figure 6b shows MR images of $SOD1^{G^{93A}}$ and Ntg mouse brains, with the Facial Nucleus region of interest (ROI) clearly paler in the $SOD1^{G^{93A}}$ mouse.

3.2.3. Whisker variables correlate well with declines in the Facial Nucleus

To examine further whether it is the decline of motor neurons in the Facial Nucleus, or the declining locomotion (pelvic muscle) that causes the changes in locomotion and whisker variables, Spearman's Rank correlations were run on the SOD1^{G93A} mouse dataset only, with all the age points included together. Scattergraphs of these correlations are presented in Figure 7. Figure 7 shows that offset and retraction velocity are both significantly correlated with the Facial Nucleus decline ($p < 0.05$). Only locomotion is correlated significantly with the declining pelvic volume ($p < 0.05$). Results from these correlation analyses can be found in the Supplementary material (Supplement 3). When the same analysis was run on the non-transgenic (Ntg) mice in the same way, the Facial Nucleus hyperintensity was not correlated to any of the whisker variables and the Pelvic Muscle volume was not correlated to locomotion velocity (Supplement 3).

While correlations cannot imply causation, retraction velocity, in particular, looks to be affected by neurodegeneration; it is correlated to hyperintensity of the facial nucleus (Figure 7i), but not to the pelvic muscle decline (Figure 7j). In addition, the muscles responsible for retraction movements seem to be most affected by the disease (Figure 3, Figure 4). Therefore, retraction velocity and offset, are likely to be directly impacted by changes in the Facial Nucleus and facial musculature in the SOD1^{G93A} mouse. Other important behavioural observations can also be seen in terms of locomotion speed, whisk frequency and whisk movement.

4. Discussion

Here, we present compelling evidence that while whisking is still present in SOD1^{G93A} mice, ALS does affect certain whisking behaviours. SOD1^{G93A} mice have longer whiskers with larger amplitudes; their whiskers are held further back and retract quicker. However, that the whiskers are still actively whisking indicates that the facial areas are relatively robust to ALS. Changes in whisker behaviour are likely to be caused by degeneration of very specific muscles, in particular the caudal, superficial extrinsic muscles (*m. Nasolabialis* and *m. Maxillolabialis*) that control retraction movements. In addition, both whisker offset and retraction velocity are correlated to the hyperintensity of the Facial Nucleus in SOD1^{G93A} mice. Other areas do change significantly throughout the progression of disease in the SOD1^{G93A} mouse, including the cerebral cortex and cerebellum. Therefore, although behavioural deficits are strongly correlated to the hyperintensity of the Facial Nucleus, this is

likely to be due to the neurodegeneration of a combination of brain structures, of which the Facial Nucleus is the final common motor path for whisker control.

Conversely, other brain areas may be able to compensate for the changes in the Facial Nucleus. Certainly, brain areas such as the basal ganglia (Huston et al. 1986; 1990; Steiner et al. 1989), superior colliculus (Triplett et al. 2012) and cortex (Glazewski et al. 2007; Rema et al. 2003) have all been found to significantly alter in structure following whisker removal or ablation of the sensory nerve. These structures are all connected to the Facial Nucleus, either directly or via other structures, and therefore, could realistically compensate for some of the effects of neurodegeneration, and contribute to the relative resistance of the facial area to neurodegeneration.

That the pelvis and locomotion behaviour are affected before, and perhaps more than the facial nucleus and whisking behaviour is an interesting finding. It has been observed previously in a limited number of muscle studies that facial muscles are more resistant than locomotion muscles (Murray et al. 2008; Valdez et al. 2012); however, most research has not considered facial muscles at all. Here it can be seen that pelvic muscles have a more marked decline (Figure 6), compared to the facial muscles (Figure 4). Valdez et al. (2012), who used SOD1^{G93A} mice as a model of aging, suggested that muscles innervated by longer motor axons, such as the hindlimbs, might be more affected by neurodegeneration than shorter axons, such as the facial muscles. It might also be that rostral areas (facial muscles) are more disease resistant than caudal areas (pelvic muscles). Indeed, Valdez et al. (2012) found that neuromuscular junctions in rostral muscles show less disease-related changes than caudal neuromuscular junctions. This might also explain why the caudal muscles of the mystacial pad (superficial extrinsic muscles) are affected more than other more rostral facial muscles, such as the deep retracting muscles and extrinsic protracting muscles (Haidarliu et al. 2010).

Not only do the limb and facial areas differ in terms of their distance from the brain, and their rostro-caudal coordinates, but the facial musculature of the mouse has a very specific architecture that might make it more resistant to muscular degeneration. The intrinsic muscles are coupled from whisker-to-whisker in the same row, like a chain (Dorfl, 1982). Therefore, degeneration of some intrinsic muscles might be compensated by others in the same row, and passively moved as part of the chain. The intrinsic muscles are those that are responsible for protraction movements, which were least affected in the SOD1^{G93A} mice in this study. In

addition, protraction movements are thought to be more actively controlled than retraction movements (Carvell and Simons 1990) as they are slower and more variable. Intrinsic muscles also have proportionally more motoneurons innervating them in the facial nucleus, than extrinsic muscles (Klein & Rhoades 2004). The superficial extrinsic muscles are, therefore, more likely to be affected by degeneration than the intrinsics as they are caudal to the pad, innervated by fewer motoneurons and not in a chain architecture. Decline of the superficial extrinsic muscles as we observed here, could cause less resistance to forward movements, hence accounting for the increase in amplitude. The animals would also have less control over retraction movements, hence causing quicker retractions, as we have seen here.

Previous studies have also found that disease progression impacts fast muscles more than slow muscles in SOD1^{G93A} mice (David et al. 2007) with fast fibres being more prone to dystrophy, denervation, and ischemia (David et al. 2007; Valdez et al. 2012). This agrees with the qualitative muscle images here (Figures 3 and 4) that show a decline in the fast, type ii muscle fibres of the superficial retracting muscles. All the muscles in the mystacial pad contain type i and type ii muscle fibers (Haidarliu et al. 2010), although the intrinsic muscles are thought to contain the highest percentage of the fast, type ii fibers (Jin et al. 2004). However, for the reasons discussed above, these muscles might be fairly resistant to degeneration.

Future work exploring whether it is the facial muscle architecture or its reduced neurodegeneration that explains the robustness of whisking protraction movements to disease progression, would be an important addition to this study. However, significant changes in whisker retractions especially, and offset, amplitude and frequency have been identified for the first time in this study. Using whisking and locomotion behaviours together could be a useful model to study disease progression and treatment. The method is non-invasive, quick, and does not require the animal to be trained, unlike other behavioural tasks, such as the rotorod test. It is worth bearing in mind that behaviour data is relatively variable, indeed there were earlier behavioural locomotion deficits observed in the SOD1^{G93A} mice in study 1 (Figure 2), which had larger sample numbers. This agrees with other observations of behavioural experiments in SOD1^{G93A} mice (Bucher 2007) and it is recommended to have large animal numbers for all preclinical animal research in ALS, according to updated guidelines (Ludolph et al. 2010).

Conclusions

Whisking is conserved during disease progression in the SOD1^{G93A} mouse ; however, specific whisker movements are affected by neurodegeneration. While the facial area is fairly resistant to ALS in the SOD1^{G93A} mouse overall, we observe some reductions in the caudal fast muscle fibers of the mystacial pad, that affects the retraction movements of the whiskers at P120. The observed changes in whisker behaviours are strongly correlated to neurodegeneration of the Facial Nucleus. We present here that whisker analyses could be used as a new behavioural model of ALS. While this model is still in an early phase of development, we think that further exploring the relationship between muscle degeneration and behaviour is a useful and important step in quantifying clinical aspects of neurodegenerative disorders, for better characterisation and treatment.

References

- Berg, R.W, & Kleinfeld, D. (2003). Rhythmic whisking by rat, retraction as well as protraction of the vibrissae is under active muscular control. *J Neurophysiol* 89: 104–117.
- Bucher, S., Braunstein, K.E., Niessen, H.G., Kaulisch, T., Neurmaier, M., Boeckers, T.M., Stiller, D. & Ludolph, A.C. (2007). Vacuolization correlates with spin–spin relaxation time in motor brainstem nuclei and behavioural tests in the transgenic G93A-SOD1 mouse model of ALS. *European Journal of Neuroscience*, 26: 1895-1901
- Carvell, G.E. & Simons, D.J. (1990). Biometric analyses of vibrissal tactile discrimination in the rat. *J. Neurosci.* 10(8):2638-48
- Chatfield, C. (2003). The analysis of time series: An introduction (6th ed.). London: Chapman and Hall
- Chiu, A.Y., Zhai, P., Dal Canto, M.C., Peters, T.M., Kwon, Y.W., Prattis, S.M. & Gurney, M.E. (1995). Age-dependent penetrance of disease in a transgenic mouse model of familial amyotrophic lateral sclerosis. *Molecular and Cellular Neuroscience*, 6:349-362

David, G., Nguyen, K. & Barrett, E.F. (2007). Early vulnerability to ischemia/reperfusion injury in motor terminals innervating fast muscles of SOD1-G93A mice. *Exp. Neurol.* 204:411-420

Dorfl, J. (1982). The musculature of the mystacial vibrissae of the white mouse. *J Anat* 135: 147–154.

Geser, F., Brandmeir, N.J., Kwong, L.K., Martinex-Lage, M., Elman, L., McCluskey, L., Xie, S.X., Lee, V. M.-Y., Trojanowski, J.Q. (2008). Evidence of Multisystem Disorder in Whole-Brain Map of Pathological TDP-43 in Amyotrophic Lateral Sclerosis. *Arch Neurol*, 65(5):636-641

Glazewski, S., Benedetti, B.L. & Barth, A.L. (2007). Ipsilateral Whiskers Suppress Experience-Dependent Plasticity in the Barrel Cortex. *J. Neurosci.* 27(14):3910-3920

Grant, R.A., Haidarliu, S., Kennerley, N.J. & Prescott, T.J. (2013). The evolution of active vibrissal sensing in mammals: evidence from vibrissal musculature and function in the marsupial opossum *Monodelphis domestica*. *J. Exp Biol.* Online

Grant, R.A., Mitchinson, B., & Prescott, T.J. (2012). The development of whisker control in rats in relation to locomotion. *Developmental Psychobiology*, 54(2):151-168

Haidarliu, S., Simony, E., Golomb, D., & Ahissar, E. (2010). Muscle architecture in the mystacial pad of the rat. *Anat. Rec.* 293: 1192-1206

Huston, J.P., Morgan, S., Lange, K.W. and Steiner, H. (1986). Neuronal plasticity in the nigrostriatal system of the rat after unilateral removal of vibrissae. *Experimental Neurology*, 93:380-389

Huston, J.P., Steiner, H., Weiler, H.-T., Morgan, S. and Schwarting, R.K.W. (1990). The basal ganglia-orofacial system: studies on neurobehavioral plasticity and sensory-motor tuning. *Neurosciences and Biobehavioral Reviews*, 14:433-446

Jin, T.E., Witzemann, V. & Brecht, M. (2004). Fiber types of the intrinsic whisker muscle and whisking behavior. *J Neurosci.* 24(13):3386-93

Klein, B.G & Rhoades, R.W. (2004). Representation of whisker follicle intrinsic musculature in the facial motor nucleus of the rat. *J. Comp Neurol.* 232(1):55-69

Klivenyi, P., Ferrante, R.J., Matthews, R.T., Bogdanov, M.B., Klein, A.M., Andreassen, O.A., Mueller, G., Wermer, M., Kaddurah-Daouk, R. & Beal, M.F. (1999) Neuroprotective effects of creatine in a transgenic animal model of amyotrophic lateral sclerosis. *Nat Med.* 5(3):347-350

Knippenberg, S., Thau, N., Dengler, R., Petri, S. (2010). Significance of behavioural tests in a transgenic mouse model of amyotrophic lateral sclerosis (ALS). *Behav. Brain Res.* 213:82-87

Ludolph, A.C., Bendotti, C., Blaugrund, E., Chio, A., Greensmith, L., Loeffler, J.P., Mead, R., Niessen, H.G., Petri, S., Pradat, P.F., Robberecht, W., Ruegg, M., Schwalenstöcker, B., Stiller, D., van den Berg, L., Vieira, F. & von Horsten, S. (2010). Guidelines for preclinical animal research in ALS/MND: A consensus meeting. *Amyotroph. Lateral Scler.* 11(1-2):38-45

Marcuzzo, S., Zucca, I., Mastropietro, A., de Rosbo, N.K., Cavalcante, P., Tartari, S., Bonanno, S., Preite, L., Mantegazza, R. & Bernasconi, P. (2011). Hind limb muscle atrophy precedes cerebral neuronal degeneration in G93A-SOD1 mouse model of amyotrophic lateral sclerosis: A longitudinal MRI study. *Exp. Neurol.* 231:30-37

Mead RJ, Bennet E, Kennerly A, Sharp P, Sunyach C, Kasher P, Berwick J, Pettmann B, Battaglia G, Azzouz M, Grierson A, Shaw PJ (2011). Optimisation of pre-clinical pharmacology studies in the SOD1G93A transgenic mouse model of Motor Neuron Disease. *PLoS One* 6(8), e23244.

Mitchinson, B., Grant, R.A., Arkley, K.P., Perkon, I., & Prescott, T.J. (2011). Active vibrissal sensing in rodents and marsupials. *Philosophical Transactions B.* 366(1581): 3037-3048

- Murray LM, Comley LH, Thomson D, Parkinson N, Talbot K, et al. (2008) Selective vulnerability of motor neurons and dissociation of pre- and post-synaptic pathology at the neuromuscular junction in mouse models of spinal muscular atrophy. *Hum. Mol. Genet.* 17: 949–962
- Nimchinsky, E.A., Young, W.G., Yeung, G., Shah, R.A., Gordon, J.W., Bloom, F.E., Morrison, J.H. & Hof, P.R. (2000). Differential Vulnerability of Oculomotor, Facial, and Hypoglossal Nuclei in G86R Superoxide Dismutase Transgenic Mice. *J. Comp. Neurol.* 416:112-125
- Paxinos, George, and Keith BJ Franklin (2008). *The Mouse Brain in Stereotaxic Coordinates, Compact: The Coronal Plates and Diagrams.* Academic Press.
- Perkon, I., Kosir, A., Itskov, P.M., Tasic, J. & Diamond, M.E. (2011). Unsupervised quantification of whisking and head movement in freely moving rodents. *J. Neurophys.* 105(4): 1950-1962
- Rema, V., Armstrong-James, M. & Ebner, F.F. (2003). Experience-Dependent Plasticity Is Impaired in Adult Rat Barrel Cortex after Whiskers Are Unused in Early Postnatal Life. *J. Neurosci.* 23(1):358-366
- Robberecht, W. & Philips, T. (2013) The changing scene of amyotrophic lateral sclerosis. *Nat Rev Neurosci.* 14(4):248-264
- Steiner, H., Weiler, H.-T., Morgan, S. and Huston, J.P. (1989). Asymmetries in crossed and uncrossed nigrostriatal projections dependent on duration of unilateral removal of vibrissae in rats. *Experimental Brain Research*, 77:421-424
- Triplett, J.W., Phan, A., Yamada, J. & Feldheim, D.A. (2012). Alignment of Multimodal Sensory Input in the Superior Colliculus through a Gradient-Matching Mechanism. *J. Neurosci.* 32(15):5264-5271
- Valdez, G., Tapia, J.C., Lichtmans, J.W., Fox, M.A. & Sanes, J.R. (2012). Shared Resistance to Aging and ALS in Neuromuscular Junctions of Specific Muscles. *PLoS ONE* 7(4): e34640

Vincent, S.B. (1912). The function of the vibrissae in the behavior of the white rat. *Behav. Monogr.* 1(5): 1-85

Weydt, P., Hong, S.Y., Kliot, M. & Moller, T. (2013). Assessing disease onset and progression in the SOD1 mouse model of ALS. *Neuroreport*, 14(7):1051-1054

Wineski, L.E. (1985) Facial morphology and vibrissal movement in the golden hamster. *J Morphol* 183: 199–217.

Wooley, C.M., Sher, R.B., Kale, A., Frankel, W.N., Cox, G.A. & Seburn, K.L. (2005). Gait analysis detects early changes in transgenic Sod1(G93A) mice. *Muscle Nerve*, 32: 43-50

Zang, D.W., Yang, Q., Wang, H.X., Egan, G., Lopes, E. & Cheema, S.S. (2004). Magnetic resonance imaging reveals neuronal degeneration in the brainstem of the superoxide dismutase 1^{G93A} ^{G1H} transgenic mouse model of amyotrophic lateral sclerosis. *European Journal of Neuroscience*, 20: 1745-1751

Acknowledgments

The authors would like to thank Dr Ben Mitchinson and Kendra Arkley, for their help and advice with data collection and whisker tracking. We are grateful to Dr Andy Grierson and Dr Richard Mead for their support. Many thanks also to Natalie Kennerley for supervising the histology work, and Graham Tinsley for microscope tips. We also acknowledge the continued support and advice from all the members of the ABRG. Video analysis was performed using the BIOTACT Whisker Tracking Tool which was jointly created by the International School of Advanced Studies, the University of Sheffield, and the Weizmann Institute of Science under the auspices of the FET Proactive project FP7 BIOTACT project (ICT 215910), which also partly funded the study. The MRI work was funded by an EPSRC/BBSRC collaborative project grant (EP/G062137/1) awarded to Dr. G. Battaglia.

FIGURE CAPTIONS

Figure 1 tracking and whisker trace examples for one SOD1^{G93A} mouse and one non-transgenic (Ntg) mouse. a) an example of whisker and head tracking for a SOD1^{G93A} mouse; b) the corresponding whisker traces (mean angular position, MAP), red is left and blue is right; c) an example of whisker and head tracking for a Ntg mouse; d) b) the corresponding whisker traces (mean angular position, MAP), red is left and blue is right.

Figure 2 Locomotion and whisking behaviours at P60, P90 and P120 for SOD1^{G93A} (solid black line) and Ntg (dashed line) mice. a) locomotion velocity; b) whisker offset; c) whisking amplitude; d) whisking frequency; e) whisker retraction velocity. Significant differences ($p < 0.05$) between SOD1^{G93A} and Ntg are denoted by the asterisk (*). All whisker variables are affected in SOD1^{G93A} mice by P120, locomotion is affected throughout.

Figure 3 Staining for Cytochrome Oxidase in Ntg (top) and SOD1^{G93A} (bottom) mice. a) entire pad staining in Ntg mouse; b) intrinsic sling muscle staining in Ntg mouse (see corresponding box in a); c) a close-up of the superficial retracting muscles (m. Nasolabialis) in Ntg mouse (see corresponding box in a); d) entire pad staining in SOD1^{G93A} mouse; e) intrinsic sling muscle staining in SOD1^{G93A} mouse (see corresponding box in a); f) a close-up of the superficial retracting muscles (m. Nasolabialis) in SOD1^{G93A} mouse (see corresponding box in a); g) an additional close-up of the superficial retracting muscles in SOD1^{G93A} mouse. Photos suggest that SOD1^{G93A} mice have decreased white muscle fibers in the superficial retracting muscles, compared to the Ntg mice.

Figure 4 superficial retracting muscles (m. Nasolabialis) in Ntg (a) and Sod1 (b) mice. The SOD1^{G93A} mice show a decline in the white muscle fibers.

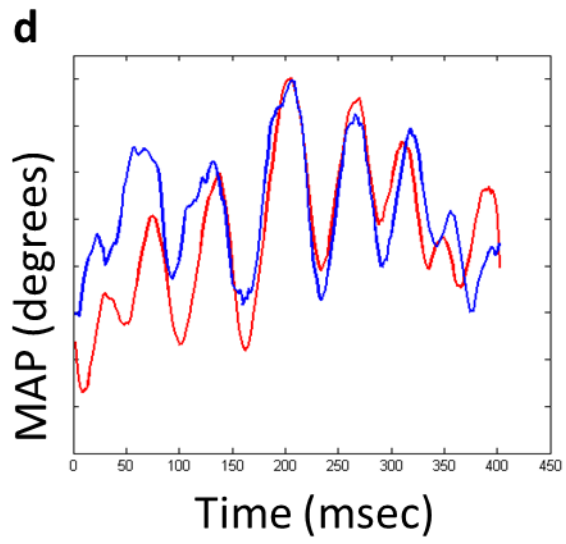
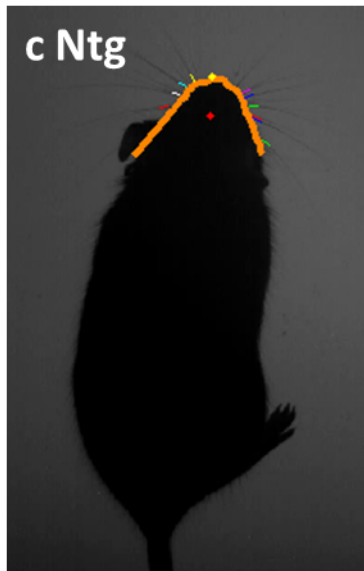
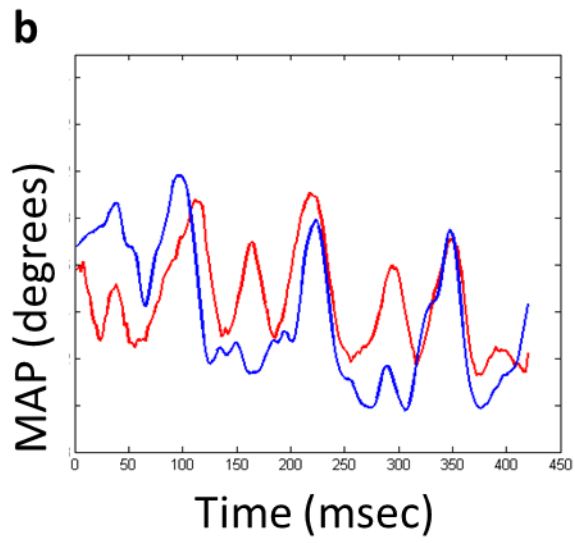
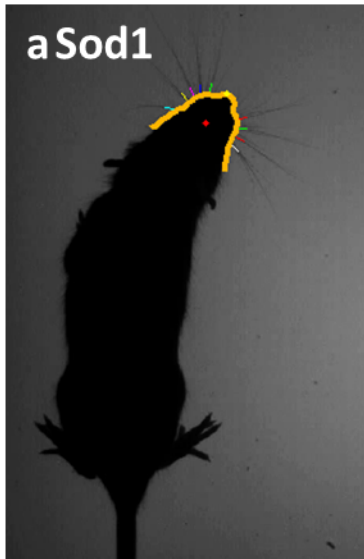
Figure 5 Locomotion and whisking behaviours at P60, P90 and P120 for Sod1 (solid black line) and Ntg (dashed line) mice. a) locomotion velocity; b) whisker offset; c) whisking amplitude; d) whisking frequency; e) whisker retraction velocity. All whisker variables are affected in SOD1^{G93A} mice by P120, locomotion is affected throughout, these results confirm earlier findings in Figure 2.

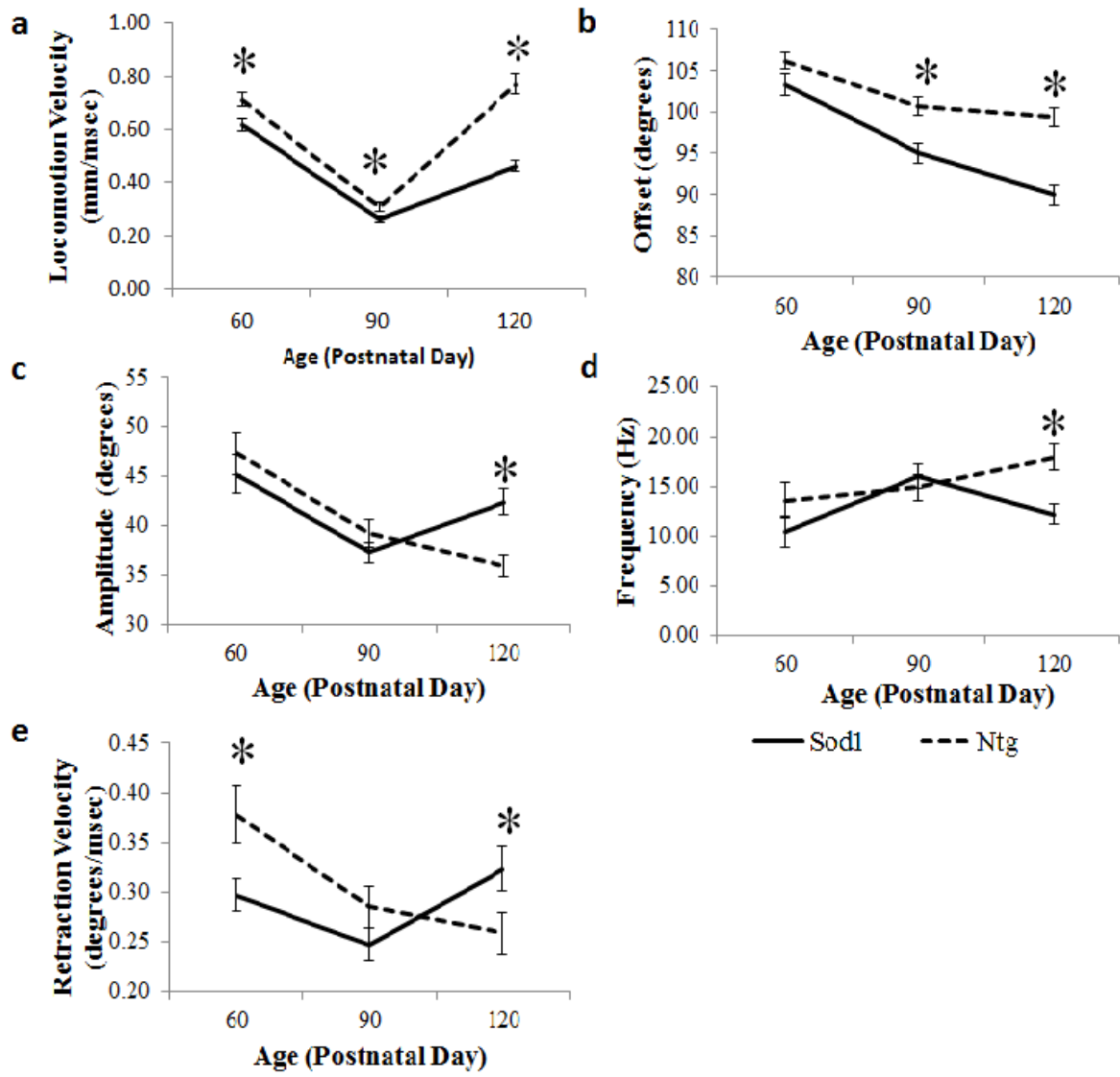
Figure 6 changes in pelvic muscle volume and Facial Nucleus MR signal in SOD1^{G93A} mice, at P30, P60, P90 and P120. a) Pelvic muscle volume decreases in SOD1^{G93A} mice, which can be seen in the graph (P30-P120) and by comparing the MR image on the right between Ntg and SOD1^{G93A} mice, which was taken at P120. b) % MR signal increases in SOD1^{G93A} mice, between the Facial Nucleus (ROI: region of interest) and the surrounding region. This can be seen in the graph (P30-P120) and by comparing the MR image on the right between Ntg and SOD1^{G93A} mice, which was taken at P120. The ROI is clearly seen in the SOD1^{G93A} mouse example.

Figure 7 Correlating whisker variables with MRI variables, % Change in Facial Nucleus MR signal (left) and Pelvic area muscle volume (right). For variables locomotion (a, b), offset (c, d), amplitude (e, f), frequency (g, h) and retraction velocity (i, j), respectively. Locomotion, offset and retraction velocity are all significantly correlated with declining Facial Nucleus signal, while only locomotion is significantly correlated to Pelvic area volume. Significant results ($p < 0.05$) are indicated by an asterisk (*). The four age points are also denoted, P30 (yellow), P60 (red), P90 (blue) and P120 (red).

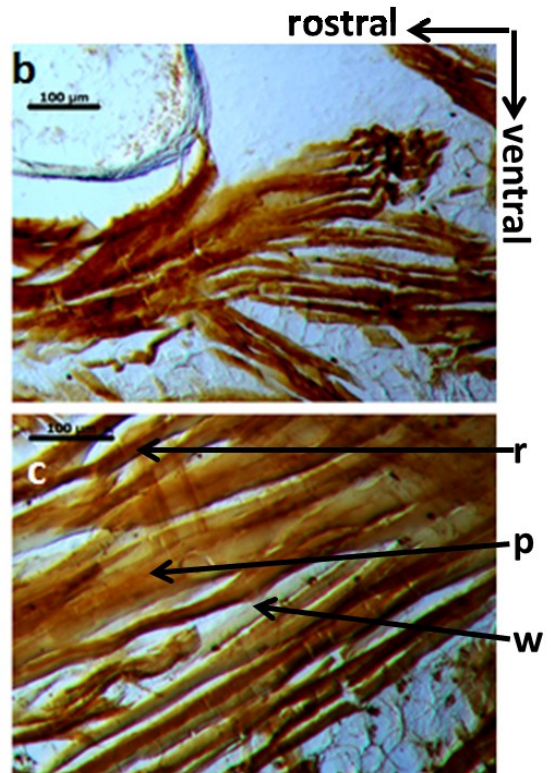
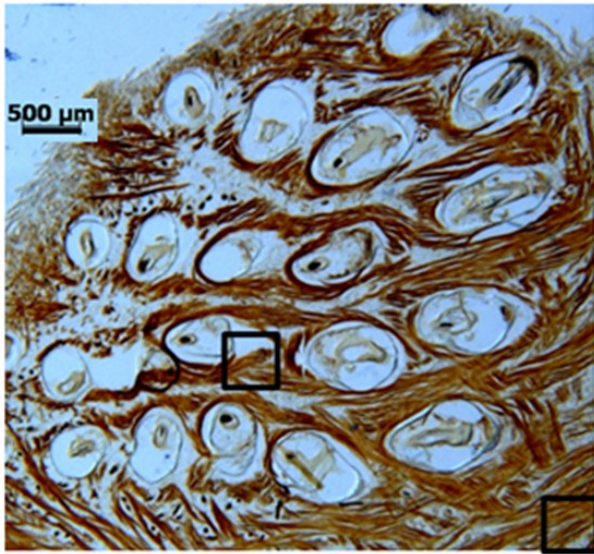
TABLE CAPTIONS

Table 1: ANOVA analysis of the locomotion and whisking variables at P120, with disease presence (Sod1 or Ntg) as the between-factor. Additional analyses conducted with mouse identity and locomotion as covariates can also be seen.

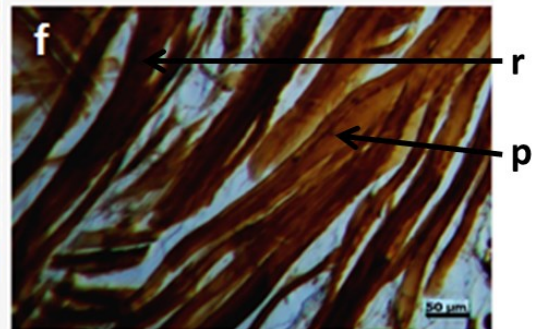
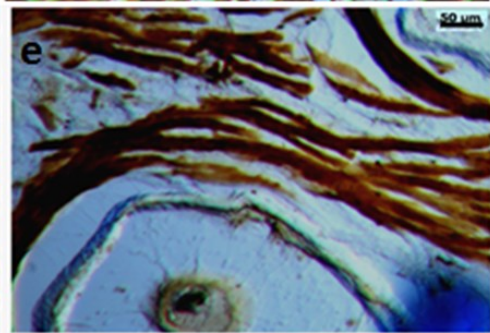
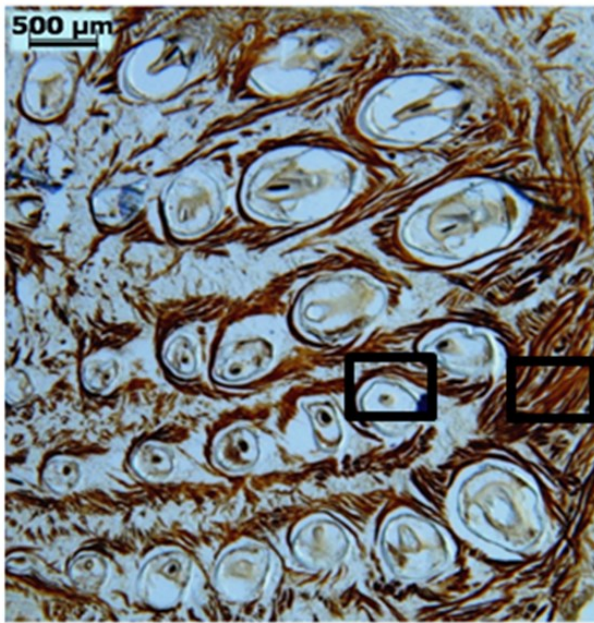




a Ntg



d Sod1



a Ntg

b Sod1

